

Optical Properties of Colloidal PbSe Nanocrystals

Hui Du,[†] Chialing Chen,[†] Rishikesh Krishnan,[‡] Todd D. Krauss,^{*,†}
Jeffrey M. Harbold,[§] Frank W. Wise,[§] Malcolm G. Thomas,[§] and John Silcox[§]

*Departments of Chemistry and Electrical and Computer Engineering,
University of Rochester, Rochester, New York 14627, and Department of
Applied Physics, Cornell University, Ithaca, New York 14853*

Received September 6, 2002; Revised Manuscript Received October 9, 2002

ABSTRACT

We present the structural and optical characterization of colloidal PbSe nanocrystals. The lowest-energy exciton transitions in these structures, with diameters between 3 and 8 nm, occur at wavelengths between 1.0 and 1.85 μm . Band-edge luminescence spectra with quantum yields as high as 80% are observed. Unexpectedly long (~ 300 ns) luminescence lifetimes are observed. These properties are promising for applications in optoelectronics and microscopy.

Colloidal II–VI and III–V semiconductor quantum dots (QDs) have attracted much attention because of their interesting electronic and optical properties and potential for a wide range of applications. For example, CdSe nanoparticles have shown potential as superior biological labels,^{1–3} improved organic–inorganic hybrid solar cells,⁴ white-light laser sources,^{5–7} and tunnel diodes,⁸ whereas InAs QDs have demonstrated their potential as near-IR emitters⁹ and as nanometer-scale components for molecular electronics.¹⁰

The exciting potential of these quantum-confined materials arises from the fact that it is possible to fabricate structures of radius R smaller than the electron–hole-pair (exciton) Bohr radius a_B . Although the exciton in II–VI and III–V QD materials can be strongly confined, there is a significant asymmetry between the individual charge carriers owing to the large difference in their effective masses. The Bohr radius of the hole in most II–VI and III–V materials is ~ 1 nm, so it is effectively impossible to achieve strong confinement of the hole.

QDs of IV–VI materials such as PbS and PbSe offer unique access to the regime of extreme quantum confinement since the electron, hole, and exciton all have relatively large Bohr radii.¹¹ In PbSe, the electron, hole, and exciton Bohr radii are 23, 23, and 46 nm, respectively. These large radii allow strong confinement to be achieved in relatively large structures. Thus, QDs of IV–VI materials may have properties reflecting all of the benefits of strong quantum confinement, with reduced influence from surface effects; for the

same level of confinement as that of QDs of II–VI or III–V materials, the surface-to-volume ratio can be quite low in IV–VI materials. Furthermore, these large Bohr radii also allow for materials to be fabricated with much stronger quantum confinement than is possible with II–VI or III–V materials.¹² Indeed, studies of extremely confined IV–VI QDs have revealed that these materials have unique vibrational modes,¹³ can exhibit extremely weak electron–phonon coupling,¹⁴ have negligible exchange and Coulomb energies,¹⁵ and can have a temperature-independent band gap.¹⁶ Lead–salt quantum dots are among the few materials that can provide size-quantized electronic transitions at technologically important infrared wavelengths. These structures may find use in optoelectronic applications as well as in biophysical applications such as fluorescence microscopy.

Despite the potential advantages of working with QDs in the extremely strong confinement limit, IV–VI QDs have received relatively little attention. This is partially due to the difficulty of synthesizing colloidal quantum dots with a well-controlled size, narrow size distribution, and well-passivated surface. Monodisperse PbS¹⁷ and PbSe¹⁸ QDs have been produced in glass hosts. However, some applications will benefit from the processability of colloidal solutions. Recently, the synthesis of high-quality colloidal PbSe QDs was reported by Murray and co-workers.¹⁹ Electron microscopy and optical absorption spectra show that monodisperse QDs of a controllable mean size were produced.

Here we describe the synthesis and characterization of colloidal PbSe quantum dots. Sizes ranging from 3 to 8 nm in diameter are produced with narrow size distributions. The ratio of quantum dot to exciton radii R/a_B is a measure of the degree of confinement and is very small: R/a_B ranges

* Corresponding author. E-mail: Krauss@chem.rochester.edu.

[†] Department of Chemistry, University of Rochester.

[‡] Department of Electrical and Computer Engineering, University of Rochester.

[§] Cornell University.

from 0.07 to 0.2 for these quantum dots. The structures exhibit clear exciton peaks in absorption and bright band-edge luminescence.

PbSe quantum dots were synthesized according to modified versions of the literature methods.¹⁹ The reaction consisted of a single-flask, single-injection synthesis based on techniques described by Murray et al.¹⁹ Trioctylphosphine (TOP) was purchased from Fluka, and all other reagents were purchased from Aldrich. For a typical synthesis, 1.5 g of lead acetate and 5.1 mL of oleic acid were dissolved in 25 mL of phenyl ether. The reaction mixture was heated to 140 °C for 1 h under stirring and under a continuous flow of nitrogen and then cooled. When the temperature of the phenyl ether solution fell below 70 °C, 12 mL of 1 M trioctylphosphine selenide (TOPSe) was added to the flask, thereby forming the molecular precursor solution. The precursor solution was subsequently loaded into a 50-mL syringe and was rapidly injected into a flask containing 40 mL of vigorously stirred phenyl ether under a continuous flow of nitrogen. The injection and growth temperature was varied from 80 to 150 °C to obtain the desired particle size. Higher injection and growth temperatures were used to prepare larger-sized QDs. After injection, the reaction mixture was maintained at the growth temperature for 5 to 10 min, and then the colloid was cooled to approximately 40 °C and stored in hexane.

The quantum dots were characterized by X-ray diffraction, scanning transmission electron microscopy (STEM), optical absorption spectroscopy, and fluorescence spectroscopy. Samples were prepared according to the following procedure. PbSe quantum dots were precipitated from hexane with a butanol/methanol mixture and centrifuged to remove excess TOP, oleic acid, and phenyl ether. After repeating this procedure twice, the solid PbSe QD pellet was dissolved in tetrachloroethylene. Provided that favorable conditions of temperature, injection, and nanocrystal growth time were employed, size-selective precipitation was not necessary to obtain narrow size distributions.

Powder X-ray diffraction was performed at room temperature on a Philips multipurpose diffractometer using Cu K α 1 radiation (0.154056 nm). Samples were prepared by evaporating several drops of the PbSe nanocrystal sample onto a special low-background X-ray sample-holder plate. STEM samples were prepared by depositing an \sim 20- μ L drop of the colloid in hexane or tetrachloroethylene on a holey carbon film on a 300-mesh copper grid. A Vacuum Generators HB501UX scanning transmission electron microscope operating at 100 keV and equipped with a high-resolution pole piece was used to acquire the STEM images. Bright-field and annular dark-field images were simultaneously acquired using software developed at Cornell University.²⁰

Absorption spectra were recorded on a Perkin-Elmer UV/vis/NIR spectrometer (Lambda 19). Fluorescence spectra and quantum yield (QY) measurements were performed on a modular research fluorescence system from Acton Research. Fluorescence was collected at a right angle to the excitation and detected with an InGaAs photodiode. For fluorescence measurements, care was taken to limit the

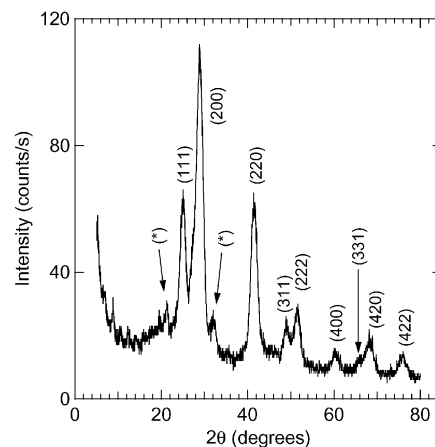


Figure 1. X-ray diffraction pattern of PbSe QDs indexed to the bulk rock salt crystal structure. The peaks labeled (*) are due to trace amounts of the unreacted precursor, lead oleate.

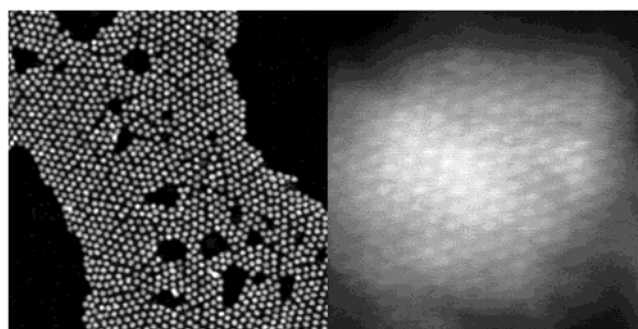


Figure 2. STEM micrographs of PbSe QDs: (left) low resolution (full scale = 320 nm) showing the ordering of an ensemble of NCs and (right) high resolution (full scale = 12.8 nm) revealing lattice imaging of the NC.

optical density to <0.1 at the lowest exciton of all samples. The laser dye IR 125 (which has a QY of 13% in dimethyl sulfoxide²¹) was used as a standard for determining the quantum yield of the PbSe quantum dots. Fluorescence decays were recorded using time-correlated single-photon counting (PicoQuant FluoTime 200). A pulsed diode laser (880-nm wavelength) was used for excitation, and a cooled Ge avalanche photodiode recorded the time-correlated signal.

PbSe quantum dots of different diameters were obtained by varying the growth temperature of the solution. Temperatures of 80 to 150 °C were used to tune the nanocrystal size continuously from 3 to 8 nm. The X-ray diffraction trace in Figure 1 exhibits clear peaks that confirm the rock salt crystal structure with the lattice constant of bulk PbSe. From the widths of the diffraction orders we estimate the nanocrystal sizes, and these are consistent with the results of electron microscopy. A typical low-magnification annular-dark-field STEM image (Figure 2 (left)) shows an ensemble of PbSe QDs assembled into a locally well-ordered close-packed array. The fact that ordered close-packed structures are observed demonstrates that the PbSe QDs have a well-controlled size and shape. Figure 2 (right) shows a high-resolution STEM image of a single PbSe QD \sim 7 nm in diameter. A hexagonal array of columns of Pb atoms is

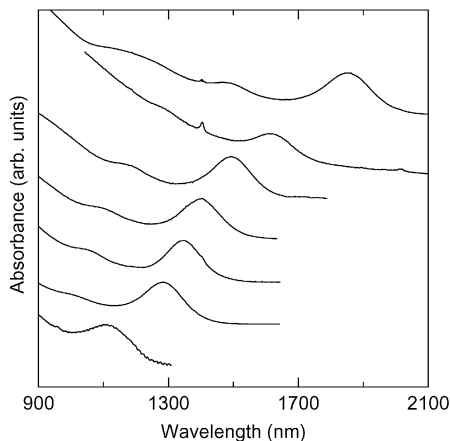


Figure 3. Linear absorption spectra of PbSe QDs ranging in size from 3 to 8 nm.

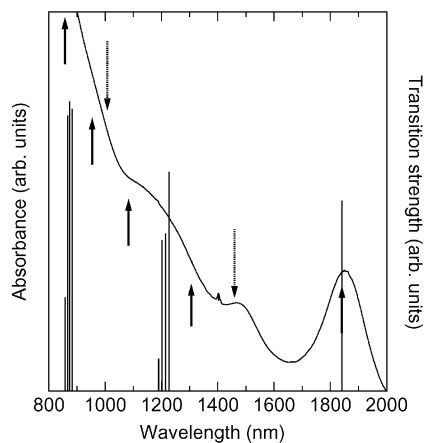


Figure 4. Linear absorption spectrum of ~ 8 -nm PbSe QDs with theoretical calculations¹⁵ of the allowed one-photon transitions (bars). The location of parity-forbidden transitions among the states found by Kang are indicated (dashed arrows), as are the new states arising from the inclusion of the anisotropy of the bulk band structure (solid arrows).²²

clearly visible in the image, showing that the synthesis produces single-crystal nanoparticles free from internal defects.

Room-temperature absorption spectra for a series of PbSe QDs are shown in Figure 3. Three distinct and sharp features are observed in most samples. As expected from quantum confinement, the onset of absorption is shifted substantially to the blue of the bulk band gap of 0.28 eV, with the 3-nm particles having a shift of 0.8 eV. From the absorption spectra we estimate a size variation of 5–10%, which is consistent with the STEM results.

The electronic structure of PbSe QDs was calculated by Kang,¹⁵ and we apply that formalism to the colloidal PbSe QDs. A calculation of the dipole-allowed optical transitions for ~ 8 -nm PbSe QDs is shown in Figure 4. The calculation is based on a bulk $\mathbf{k}\cdot\mathbf{p}$ Hamiltonian with all parameters determined by experiment and accounts for the correct symmetry of the band-edge Bloch functions. The predictions of this calculation agree very well with the first and third transition peaks in the measured absorption spectra, although a systematic deviation between the predicted and measured

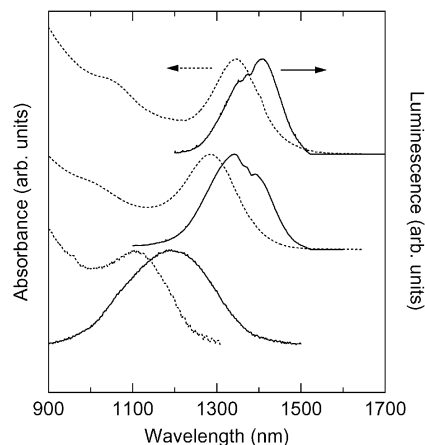


Figure 5. Band-edge luminescence from PbSe QDs excited at (bottom to top) 740, 990, and 990 nm. The measured quantum yields ranged from 12 to 81%.

energies occurs for diameters < 5 nm.¹⁸ However, the second peak, which has substantial oscillator strength, is not accounted for by Kang's theory. This situation was encountered in the study of PbS and PbSe QDs in glass. Two possible origins of the second peak have been proposed. The first is that the peak is the result of $1p_h - 1s_e$ and $1s_h - 1p_e$ transitions, which are formally parity-forbidden. Softening of the parity selection rule would allow new transitions among the states found by Kang's calculations. Another possible explanation is that the anisotropy of the bulk band structure produces new states not found by Kang.²² An analysis of the transitions that we observe in colloidal PbSe QDs does not allow a decisive assignment of the second absorption peak. However, the observed transition energies seem to favor the explanation based on the occurrence of parity-forbidden transitions among the states identified by Kang (see Figure 4).

Room-temperature photoluminescence from the PbSe QDs is bright and dominated by band-edge recombination as suggested by the small Stokes shifts (40–90 meV) in Figure 5. The spectral bandwidth of the luminescence is comparable to that of the absorption peaks, which suggests that the bandwidth is a consequence of the particle-size distribution. We do not believe that the small structures observed just below 1400 nm are intrinsic to the nanocrystals. Luminescence from deep traps, typically observed as a weak, broad, and highly Stokes-shifted emission, was never observed. Photoluminescence quantum yields at room temperature ranged between 12 and 81%. It is significant that no inorganic surface passivation, such as capping with a semiconductor shell,^{24–26} was required to obtain these quantum efficiencies that are as high as 81%. The large variation in the photoluminescence quantum yield could be caused by differences in the surface reconstruction due to when the reaction was terminated. For instance, in CdSe QDs, the photoluminescence quantum yield shows a significant variation over the course of the synthesis because of differences in optimal surface reconstruction during QD growth.²⁷

For luminescence measurements, the nanocrystals were excited well above the lowest exciton transition, so the Stokes shift cannot be interpreted directly in terms of the homoge-

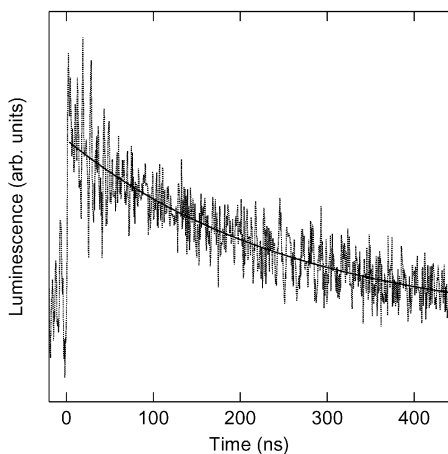


Figure 6. Luminescence decay for 3-nm PbSe QDs and a single-exponential fit to the data (250-ns time constant). The instrument response to the excitation pulse is much shorter than the measured decay (1.1 ns fwhm).

neous spectrum and intrinsic nanocrystal properties. Nevertheless, the observation of a significant Stokes shift for the ensemble luminescence does suggest one in the single-particle spectrum. This may arise from the vibronic nature of the transitions; although the coupling of excitons to optical phonons is expected to be very weak in PbSe, phonon-assisted transitions may be strong owing to non-Franck–Condon effects.²³ Further work is planned to understand the observed Stokes shift.

Fluorescence decays were recorded at the peak emission wavelength for each sample. A typical decay is shown in Figure 6 and exhibits a time constant of 250 ns. There is a trend of increasing decay time with increasing QD size; for the samples shown in Figure 5, the lifetimes are 250 ± 10 ns, 330 ± 10 ns, and 360 ± 60 ns. The observed decay times are longer than expected for a dipole transition but shorter than expected for trap-related emission. In any case, the high quantum yields and small Stokes shifts argue against emission from traps contributing significantly to the observed spectra. A straightforward calculation of the transition dipole of the lowest exciton in PbSe QDs yields a radiative lifetime on the order of nanoseconds. Dielectric screening would be expected to increase the lifetime by as much as 2 orders of magnitude if the bulk dielectric constants of PbSe are assumed. However, it is not clear that the bulk material parameters are relevant to the description of the nanocrystals. More work is needed to resolve this issue, which will have major implications for the use of PbSe QDs in applications.²⁸

In conclusion, we find that colloidal PbSe QDs synthesized following the procedure of Murray et al. exhibit excellent properties. These structures are comparable in quality to the best II–VI and III–V nanocrystals. They can be made to be very monodisperse and to offer high photoluminescence quantum yields. As is the case with lead–salt QDs in glass hosts, not all of the observed optical transitions are understood. In addition, unexpectedly slow luminescence decays are observed. Work is in progress to address these issues.

Acknowledgment. We thank Lewis Rothberg for the loan of equipment, Christine Pratt and Stephen Burns for help

with the X-ray analysis, and Christopher Murray, Kyung-Sang Cho, and Stephen O’Brien for assistance with the PbSe QD synthesis. This work was supported in part by the Army Research Office, the Center for Nanoscale Systems through the Nanoscale Science and Engineering Initiative of the National Science Foundation, award number EEC-0117770, and the New York State Office of Science, Technology, and Academic Research. This work made use of the UHV-STEM, one of the Cornell Center for Materials Research Shared Experimental Facilities, supported through the National Science Foundation Materials Research Science and Engineering Centers program (DMR-0079992). The HB501UX UHV-STEM was acquired through the National Science Foundation (grant DMR-8314255).

References

- (1) Bruchez, M., Jr.; Moronne, M.; Gin, P.; Weiss, S.; Alivisatos, A. P. *Science (Washington, D.C.)* **1998**, *281*, 2013.
- (2) Chan, W. C.; Nie, S. M. *Science (Washington, D.C.)* **1998**, *281*, 2013.
- (3) Mattoussi, H.; Mauro, J. M.; Goldman, E. R.; Anderson, G. P.; Sundar, V. C.; Mikulec, F. V.; Bawendi, M. G. *J. Am. Chem. Soc.* **2000**, *122*, 12141.
- (4) Huynh, W. U.; Dittmer, J. J.; Alivisatos, A. P. *Science (Washington, D.C.)* **2002**, *295*, 2425.
- (5) Klimov, V. I.; Mikhailovsky, A. A.; Xu, S.; Malko, A.; Hollingsworth, J. A.; Leatherdale, C. A.; Eisler, H.; Bawendi, M. G. *Science (Washington, D.C.)* **2000**, *290*, 314.
- (6) Malko, A.; Mikhailovsky, A. A.; Petruska, M. A.; Hollingsworth, J. A.; Htoon, H.; Bawendi, M. G. *Appl. Phys. Lett.* **2002**, *81*, 1303.
- (7) Kazes, M.; Lewis, D. Y.; Ebenstein, Y.; Mokari, T.; Banin, U. *Adv. Mater.* **2002**, *14*, 317.
- (8) Kim, S. H.; Markovich, G.; Rezvani, S.; Choi, S. H.; Wang, K. L.; Heath, J. R. *Appl. Phys. Lett.* **1999**, *74*, 317.
- (9) Tesster, N.; Medvedev, V.; Kazes, M.; Kan, S.; Banin, U. *Science (Washington, D.C.)* **2002**, *295*, 1506.
- (10) Banin, U.; Cao, Y.; Katz, D.; Millo, O. *Nature (London)* **1999**, *400*, 542.
- (11) Efros, A. L.; Efros, A. L. *Sov. Phys.—Semiconductors* **1982**, *16*, 772.
- (12) Wise, F. W. *Acc. Chem. Res.* **2000**, *33*, 773.
- (13) Krauss, T. D.; Wise, F. W.; Tanner, D. B. *Phys. Rev. Lett.* **1996**, *76*, 1376.
- (14) Krauss, T. D.; Wise, F. W. *Phys. Rev. Lett.* **1997**, *79*, 5102.
- (15) Kang, I.; Wise, F. W. *J. Opt. Soc. Am. B* **1997**, *14*, 1632.
- (16) Olkhovets, A.; Hsu, R.-C.; Lipovskii, A.; Wise, F. W. *Phys. Rev. Lett.* **1998**, *81*, 3539.
- (17) Borrelli, N. F.; Smith, D. W. *J. Non-Cryst. Solids* **1994**, *180*, 25.
- (18) Lipovskii, A.; Kolobkova, E.; Petrikov, V.; Kang, I.; Olkhovets, A.; Krauss, T. D.; Thomas, M.; Silcox, J.; Wise, F. W.; Shen, Q.; Kycia, S. *Appl. Phys. Lett.* **1997**, *71*, 3406.
- (19) Murray, C. B.; Sun, S.; Gaschler, W.; Doyle, H.; Betley, T. A.; Kagan, C. R. *IBM J. Res. Dev.* **2001**, *45*, 47.
- (20) Kirkland, E. J. *Ultramicroscopy* **1990**, *32*, 349.
- (21) Benson, R. C.; Kues, H. A. *J. Chem. Eng. Data* **1977**, *22*, 379.
- (22) Andreev, A. D.; Lipovskii, A. A. *Phys. Rev. B: Condens. Matter* **1999**, *59*, 15402.
- (23) Pokatilov, E. P.; Klimin, S. N.; Fomin, V. M.; Devreese, J. T.; Wise, F. W. *Phys. Rev. B: Condens. Matter* **2002**, *65*, 075316.
- (24) Hines, M. A.; Guyot-Sionnest, P. *J. Phys. Chem.* **1996**, *100*, 468.
- (25) Dabbousi, B. O.; Rodriguez-Viejo, J.; Mikulec, F. V.; Heine, J. R.; Mattoussi, H.; Ober, R.; Jensen, K. F.; Bawendi, M. G. *J. Phys. Chem. B* **1997**, *101*, 9463.
- (26) Peng, X. G.; Schlamp, M. C.; Kadavanich, A. V.; Alivisatos, A. P. *J. Am. Chem. Soc.* **1997**, *119*, 7019.
- (27) Qu, L.; Peng, X. G. *J. Am. Chem. Soc.* **2002**, *124*, 2049.
- (28) Since the submission of this paper, we have learned that a detailed calculation of dielectric screening does account quantitatively for the $\sim 0.1 \mu\text{s}$ fluorescence decay times: Wehrenberg, B. L.; Wang, C.; Guyot-Sionnest, P. *J. Phys. Chem. B* **2002**, *106*, 10634.

NL025785G